

sure in such a region is uniform, the center of pressure of the j th strip is given by

$$\bar{x}_j' = \left[(C_{p4} - C_{p1})\ell_{Lj} \left(x_{pj}' + \frac{\ell_{Lj}}{2} \right) + (C_{p5} - C_{p2})\ell_{Mj} \left(x_{pj}' + \ell_{Lj} + \frac{\ell_{Mj}}{2} \right) + (C_{p6} - C_{p3})\ell_{Tj} \left(x_{pj}' + \ell_{Lj} + \ell_{Mj} + \frac{\ell_{Tj}}{2} \right) \right] / [(C_{p4} - C_{p1})\ell_{Lj} + (C_{p5} - C_{p2})\ell_{Mj} + (C_{p6} - C_{p3})\ell_{Tj}]$$

where ℓ_{Lj} , ℓ_{Mj} , and ℓ_{Tj} are local airfoil-strip chords defined in Fig. 2. Hence, the strip pitching moment about the Y' axis, the strip rolling moment about the X' axis, and the strip yawing moment about the Z' axis are, respectively,

$$M'_{pj} = -F'_{Nj}\bar{x}_j', \quad M'_{Rj} = F'_{Nj}y_j', \quad M'_{Yj} = -F'_{Aj}y_j'$$

Summing j over all of the strips of a fin, one obtains for a fin

$$F'_N = \sum_{j=1}^n F'_{Nj}, \quad F'_L = \sum_{j=1}^n F'_{Lj}$$

$$F'_A = \sum_{j=1}^n F'_{Aj}, \quad F'_D = \sum_{j=1}^n F'_{Dj}$$

$$M'_p = \sum_{j=1}^n M'_{pj}, \quad M'_R = \sum_{j=1}^n M'_{Rj}, \quad M'_Y = \sum_{j=1}^n M'_{Yj}$$

The center-of-pressure coordinates are then

$$\bar{X}' = M'_p / F'_N, \quad \bar{Y}' = M'_R / F'_N$$

Transforming back to the XYZ system by Eq. (1), the force and the moment on a fin have, respectively, the components

$$\begin{bmatrix} F_A \\ F_S \\ F_N \end{bmatrix} = [A] \begin{bmatrix} F'_A \\ 0 \\ F'_N \end{bmatrix} = \begin{bmatrix} F'_N \sin \delta + F'_A \cos \delta \\ \sin \Gamma (F'_A \sin \delta - F'_N \cos \delta) \\ \cos \Gamma (F'_N \cos \delta - F'_A \sin \delta) \end{bmatrix}$$

$$\begin{bmatrix} M_R \\ M_p \\ M_Y \end{bmatrix} = [A] \begin{bmatrix} M'_R \\ M'_p \\ M'_Y \end{bmatrix} = \begin{bmatrix} M'_R \cos \delta + M'_Y \sin \delta \\ M'_p \cos \Gamma + \sin \Gamma (M'_R \sin \delta - M'_Y \cos \delta) \\ M'_p \sin \Gamma + \cos \Gamma (M'_Y \cos \delta - M'_R \sin \delta) \end{bmatrix}$$

Obviously, the fin dihedral angle Γ causes a side force F_S to the vehicle. Note that F'_A and F'_N are also Γ -dependent. Thus, the task of minimizing or eliminating F_S is very much involved in hypersonic flow conditions. Furthermore, note that in hypersonic flows it is difficult to decouple the roll forcing moment and the roll damping moment, or the pitch forcing moment and the pitch damping moment, in general.

The associated aerodynamic coefficients are, respectively, Lift coefficient:

$$C_N = (F_N \cos \alpha - F \sin \alpha) / A_r$$

Wave drag coefficient:

$$C_{DW} = (F_N \sin \alpha + F_A \cos \alpha) / A_r$$

Pitching moment coefficient:

$$C_m = M_p / A_r L_r$$

Rolling moment coefficient:

$$C_l = M_R / A_r L_r$$

where A_r is the reference area and L_r is the reference length.

The preceding analysis is for one fin panel. The aerodynamic characteristics for multiple fin panels can be obtained

by summing corresponding aerodynamic characteristics over all fins.

Acknowledgment

This work is partially sponsored by NSC 83-0424-E006-088. The author is indebted to D. N. Fan of Howard University for his encouragement and guidance during the course of this work.

References

- 1Eggers, A. J., Jr., Syvertson, C. A., and Kraus, S., "A Study of Inviscid Flow about Airfoils at High Supersonic Speeds," NACA Rept. 1123, 1953.
- 2Tsien, H. S., "Similarity Laws of Hypersonic Flows," *Journal of Mathematics and Physics*, Vol. 25, No. 3, 1946, pp. 247-251.
- 3Linnell, R. D., "Two-Dimensional Airfoils in Hypersonic Flows," *Journal of Aerospace Science*, Vol. 16, No. 1, 1949, pp. 22-30.
- 4Barrowman, J. S., "The Practical Calculation of the Aerodynamic Characteristics of Slender Finned Vehicles," M.S. Thesis, Catholic Univ. of America, Washington, DC, 1967.

Jerry M. Allen
Associate Editor

Columbus: To Mars with Solar-Electric Propulsion

James A. Martin* and Ricky A. Wallace†
University of Alabama, Tuscaloosa, Alabama 35487

Introduction

HUMAN travel to Mars is being considered as part of the space exploration initiative. Nuclear propulsion appears to have several benefits, but the problem of launching concentrated fissionable material into orbit and starting a reactor in a low-Earth orbit may prove too difficult to be solved in a society that is increasingly concerned with safety and ecology. Chemical propulsion leads to very massive vehicles when the desired mission design includes a rapid transfer between planets to minimize radiation damage and also includes a long stay at Mars to allow the crew to recover from the flight out before the return flight. Solar-electric propulsion offers a reasonable alternative, but it also has problems. Assembling a large array at a low-Earth-orbit node is difficult, and the long trip time from the assembly orbit to the high-Earth orbit where the crew would join the main vehicle leads to awkward mission planning.

Contents

A design for a human trip to Mars using solar-electric propulsion is proposed. The key feature of this design is that the solar array is divided into three identical parts. Each part carries cargo to a rendezvous point. Because each of the three parts carries a different cargo mass, they can be launched from the low-Earth-orbit assembly point at different times and all arrive at the rendezvous point at the same time.

Received Nov. 21, 1991; revision received April 20, 1992; accepted for publication May 11, 1992. Copyright © 1992 by J. A. Martin. Published by the American Institute of Aeronautics and Astronautics, Inc., with permission.

*Associate Professor, Department of Aerospace Engineering. Associate Fellow AIAA.

†Graduate Student, Department of Aerospace Engineering. Member AIAA.

Columbus is a design for a mission to Mars that uses solar-electric propulsion that avoids the major problems. The key feature is that the solar array needed for the interplanetary leg is divided into three parts for the Earth spiral. The three parts carry unmanned cargo to the high-Earth-orbit rendezvous point. The three cargo packages are not equal in mass. The package launched first is heaviest and thus requires the longest time to travel to the rendezvous point, and the package launched last requires the shortest time for the spiral. When the three packages arrive at the rendezvous point, the human crew arrives in a small vehicle with chemical propulsion.

Figure 1 shows the assembled Columbus vehicle, with the three large solar array parts joined, looking at the planform from the illuminated side. Each array has a thruster package, shown as a square above the array. A major structural keel is shown running from the point where the arrays join and passing under the thruster to the outer edge of each array. Figure 2 shows the side view of one part, where the crew module is visible. The truss carrying the solar array is the long horizontal linear framework. Both the top and bottom thruster packages are visible on booms above and below the solar array. The crew modules are located near the point where the three solar arrays attach, and tunnels provide access among them during the flight.

The time line for the mission is shown in Fig. 3. The first package (Pinta) is assembled from five launches of a heavy-lift vehicle and then starts to spiral from Earth. The second package (Nina) is assembled from the next three launches. The final package (Santa Maria) requires only two launches. After the crew joins the Columbus at the rendezvous point, the Mars leg starts.

The Columbus design provides for a crew of six to travel to Mars on a 1000-day conjunction-class mission. The total mass that would depart from low-Earth orbit was found to be 536×10^3 kg. Dividing the solar array into three parts appears to have several

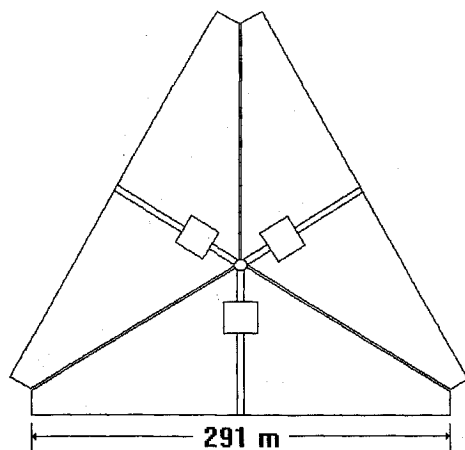


Fig. 1 Top view of Columbus.

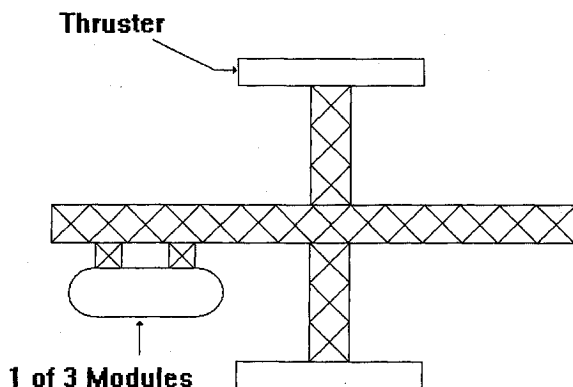


Fig. 2 Side view of one part of Columbus.

MILESTONE ITEMS	2019	2020
PINTA CONSTRUCTION	▽ ▽ ▽ ▽ ▽	
LAUNCHES 1 TO 5	▽ ▽ ▽ ▽ ▽	
PINTO TO HIGH EARTH ORBIT	▽ ▽ ▽ ▽ ▽	
NINA CONSTRUCTION	▽ ▽ ▽	
LAUNCHES 6 TO 8	▽ ▽ ▽	
NINA TO HIGH EARTH ORBIT	▽ ▽ ▽	
SANTA MARIA CONSTRUCTION	▽ ▽ ▽	
LAUNCHES 9 TO 10	▽ ▽ ▽	
SANTA MARIA TO HIGH EARTH ORBIT	▽ ▽ ▽	
CREW AT SPACE STATION	▽ ▽ ▽	
CREW TO HIGH EARTH ORBIT	▽ ▽ ▽	
HELIOCENTRIC LEG TO MARS	▽ ▽ ▽	

Fig. 3 Timeline for the Columbus mission.

advantages. The requirements of the node are minimized. The problems caused by the Earth spiral time are reduced.

Acknowledgments

The authors of the full paper deserve the credit for this study. They were the undergraduate design class of the Department of Aerospace Engineering of the University of Alabama in the spring of 1991. They were Scottie Austin, Kristina Bailey, Travis Dooley, Stephen Fordyce, Elizabeth Huskey, Patrick Kelley, Jim Neidhoefer, Richard Sheppard, Kevin Shultz, Ricky Wallace, Chris Weekley, and David Williams.

Antoni K. Jakubowski
Associate Editor

Deployed High-Temperature Superconducting Coil Magnetic Shield

Erik J. Hilinski* and F. Hadley Cocks†
Duke University, Durham, North Carolina 27706

Introduction

IN any manned space mission that lasts for an extended period of time and involves travel beyond the magnetosphere, the danger posed by radiation becomes of tantamount importance.^{1,2} Radiation shielding must be considered for a permanently manned lunar base or a manned expedition to Mars. The radiation hazard that will be encountered during

Received April 21, 1992; revision received June 12, 1992; accepted for publication June 18, 1992. Copyright © 1992 by the American Institute of Aeronautics and Astronautics, Inc. All rights reserved.

*Graduate Student, Department of Mechanical Engineering and Materials Science; currently at Case Western Reserve University, Cleveland, OH 44106.

†Professor, Department of Mechanical Engineering and Materials Science.